**Atmospheric
Chemistry
and Physics**

Constraining tropospheric mixing timescales using airborne observations and numerical models

P. Good[1], **C. Giannakopoulos**[1], **F. M. O'Connor**[2], **S. R. Arnold**[3], **M. de Reus**[4], **and H. Schlager**[5]

[1]National Observatory of Athens, Greece
[2]Centre for Atmospheric Science, Cambridge, UK
[3]School of the Environment, University of Leeds, UK
[4]Max-Planck-Institute for Chemistry, Atmospheric Chemistry Department, Mainz, Germany
[5]German Aerospace Center, Institute of Atmospheric Physics, Oberpfaffenhofen, Germany

Abstract. A technique is demonstrated for estimating atmospheric mixing time-scales from in-situ data, using a Lagrangian model initialised from an Eulerian chemical transport model (CTM). This method is applied to airborne tropospheric CO observations taken during seven flights of the Mediterranean Intensive Oxidant Study (MINOS) campaign, of August 2001. The time-scales derived, correspond to mixing applied at the spatial scale of the CTM grid. They are relevant to the family of hybrid Lagrangian-Eulerian models, which impose Eulerian grid mixing to an underlying Lagrangian model. The method uses the fact that in Lagrangian tracer transport modelling, the mixing spatial and temporal scales are decoupled: the spatial scale is determined by the resolution of the initial tracer field, and the time scale by the trajectory length. The chaotic nature of lower-atmospheric advection results in the continuous generation of smaller spatial scales, a process terminated in the real atmosphere by mixing. Thus, a mix-down lifetime can be estimated by varying trajectory length so that the model reproduces the observed amount of small-scale tracer structure. Selecting a trajectory length is equivalent to choosing a mixing timescale. For the cases studied, the results are very insensitive to CO photochemical change calculated along the trajectories. That is, it was found that if CO was treated as a passive tracer, this did not affect the mix-down timescales derived, since the slow CO photochemistry does not have much influence at small spatial scales. The results presented correspond to full photochemical calculations. The method is most appropriate for relatively homogeneous regions, i.e. it is not too important to account for changes in aircraft altitude or the positioning of stratospheric intrusions, so that small scale structure is easily distinguished. The chosen flights showed a range of mix-down time upper limits: a very short timescale of 1 day for 8 August, due possibly to recent convection or model error, 3 days for 3 August, probably due to recent convective

and boundary layer mixing, and 6–9 days for 16, 17, 22a, 22c and 24 August. These numbers refer to a mixing spatial scale of 2.8°, defined here by the resolution of the Eulerian grid from which tracer fields were interpolated to initialise the Lagrangian model. For the flight of 3 August, the observed concentrations result from a complex set of transport histories, and the models are used to interpret the observed structure, while illustrating where more caution is required with this method of estimating mix-down lifetimes.

1 Introduction

Mixing has been identified many times as having significant influence on constituent evolution both in the stratosphere and troposphere, and some progress has been made in characterising its effects (e.g. Plumb and Ko, 1992; Plumb et al., 2000; Pierce et al., 1994; Haynes and Shuckburgh, 2000a,b; Tan et al., 1998; Wild et al., 1996; Methven et al., 2003; Lee et al., 2001; Morgenstern and Carver, 1999). Observation of long range tropospheric pollution transport has given some idea about how long features can retain their identity in the troposphere. On the other hand many studies using Lagrangian trajectory models, which do not explicitly simulate mixing as a process, have shown success in reproducing observed high resolution structure when forced by analysed meteorology (e.g. Sutton et al., 1994; O'Neill et al., 1994; Plumb et al., 1994; Manney et al., 1995; Dragani et al., 2002; Methven and Hoskins, 1999; Methven et al., 2001; Evans et al., 2000), although Lagrangian transport does not always improve simulated small-scale structure (e.g. Fairlie et al., 1997; Dragani et al., 2002). Dragani et al. (2002) in particular found that reverse domain filling trajectories showed significant improvement, over the use of analysed PV, in the simulation of in-situ stratospheric data, but only when there was small scale structure observed. They highlight the treatment of mixing as an area requiring further study.

A family of hybrid Lagrangian-Eulerian (e.g. Stevenson et al., 1998; Reithmeier and Sausen, 2002; Fairlie et al., 1999) and related (McKenna et al., 2002) models are emerging, which aim to use the advantages of the Lagrangian approach, but impose a form of Eulerian mixing between trajectories. The spatial scale of the mixing must be large enough to cover more than one trajectory. The imposed mixing time-scale is a free parameter in these models. Estimation of appropriate mixing time-scales is difficult, because it depends on the unresolved small-scale tracer structure (see e.g. Nakamura, 1996, 2001). Some use shear-dependent parameterisations (Walton et al., 1988), but this has the disadvantage of enhancing mixing across wind jets such as the stratospheric vortex-dynamical features that are known to act as lateral transport barriers (e.g. Haynes and Shuckburgh, 2000a). Mostly, a mixing time-scale is chosen such that the model behaves reasonably. This work demonstrates one method for constraining mixing time-scales, using a Lagrangian model initialised from an Eulerian CTM to model in-situ CO observations taken over the eastern Mediterranean during the MINOS campaign of August 2001.

Lagrangian tracer-advection models are generally described as including no mixing processes. However in most applications tracer mixing is implicitly included through their initialization from low resolution gridpoint fields. That is, when a Lagrangian calculation is initialised with low-resolution, spatially averaged tracer fields, a form of mixing is automatically included in the final product of the calculation. Typical initializations are PV from analysed winds (e.g. O'Neill et al., 1994), satellite data (e.g. Sutton et al., 1994) and chemical transport models (e.g. Methven et al., 2001). The mixing spatial scale is determined by the initialization, in particular by the resolution of the gridpoint fields. The mixing time-scale corresponds to the trajectory length. Thus choosing a trajectory length is equivalent to selecting a mix-down lifetime (Thuburn and Tan, 1997, discuss mix-down lifetimes).

The basic method of this work is to choose a mix-down lifetime by comparing Lagrangian model results of varying trajectory durations with in-situ observations, for a long lived tracer. Since tracer advection continually produces smaller and smaller spatial scales, a trajectory duration, t_m, can be chosen such that the model reproduces the amount of small-scale structure in the observations. That is, t_m may be chosen such that for trajectories longer than t_m the model overestimates the small-scale structure, while for trajectories shorter than t_m, the model underestimates the amount of small-scale structure. If the observations show a lot of small-scale structure, then it might in general be expected that longer trajectories would be required for advection to reproduce this, so t_m will tend to be long. On the other hand, if the observations are very homogeneous, then it is likely that only relatively short trajectories will reproduce the observed small-scale structure, so t_m will be correspondingly short. A numerical model is required to quantify this for each set of observations.

The choice of t_m is made with most confidence if the region studied is relatively homogeneous, apart from the small-scale structure. That is, if neither accounting for changes in aircraft altitude, nor the positioning of stratospheric intrusions are too important, so that small scale structure is easily distinguished. Say the tracer initialization is a reasonable low-resolution approximation to the real-atmosphere equivalent over the spatial scale d_m, where d_m is a vector defining the grid resolution of the tracer initialization. In that case, t_m estimates the mix-down lifetime that should be imposed, over the spatial scale d_m, for a hybrid Lagrangian-Eulerian model to reproduce the amount of small-scale structure observed in the real atmosphere. If the advective dispersion of the trajectories is realistic, then the result is an estimate of mix-down lifetime in the real atmosphere.

Convection is of course in general a significant problem in the interpretation of trajectory calculations. Convection may be viewed as a local column of rising air which entrains and mixes turbulently with the surroundings, being progressively diluted as it ascends. Higher up in the column, the proportion of air originating from low level is smaller than lower down in the column. Hence, convection can increase tracer gradients with respect to air isolated from the convective column by raising possibly polluted air from low level, while the turbulent mixing reduces tracer gradients on a more local scale. For either of these processes to affect the results of the current study, they would have to either increase or decrease the amount of small-scale tracer structure consistently across the majority of the the air sampled. It is possible for a flight to sample predominantly air emerging from a single extended convective region. In this case, the small-scale structure can be reduced due to turbulent convective mixing. Alternatively a flight might sample both air from a large convective region and air which has not seen recent convection, brought together by advective stirring. In this case, the small-scale structure could be enhanced, since the air from the convective region may contain air from a polluted boundary layer. To mitigate these effects and other model errors, extended flight segments and a large number of trajectories – 100–200 – are used to extract each mixdown time-scale. In addition, it is important that results from multiple flights are examined, to minimise the risk of the conclusions being strongly influenced in these ways. That is, several flights should be examined to gain a general idea of mixing timescales typical of the region and time of year.

Physical interpretation of the mix-down lifetime is restricted since the mechanism for mixing in the real atmosphere differs from that in the models described here. In the models, mixing is applied at the large scale, d_m, and is then stretched to small scale by Lagrangian advection. In the real atmosphere advection stretches large features, then mixing occurs at small scales. The numerical model approach of large scale mixing is dictated by computational limitations. However, it appears that this approach can be reasonable in some situations, since Lagrangian models initialised
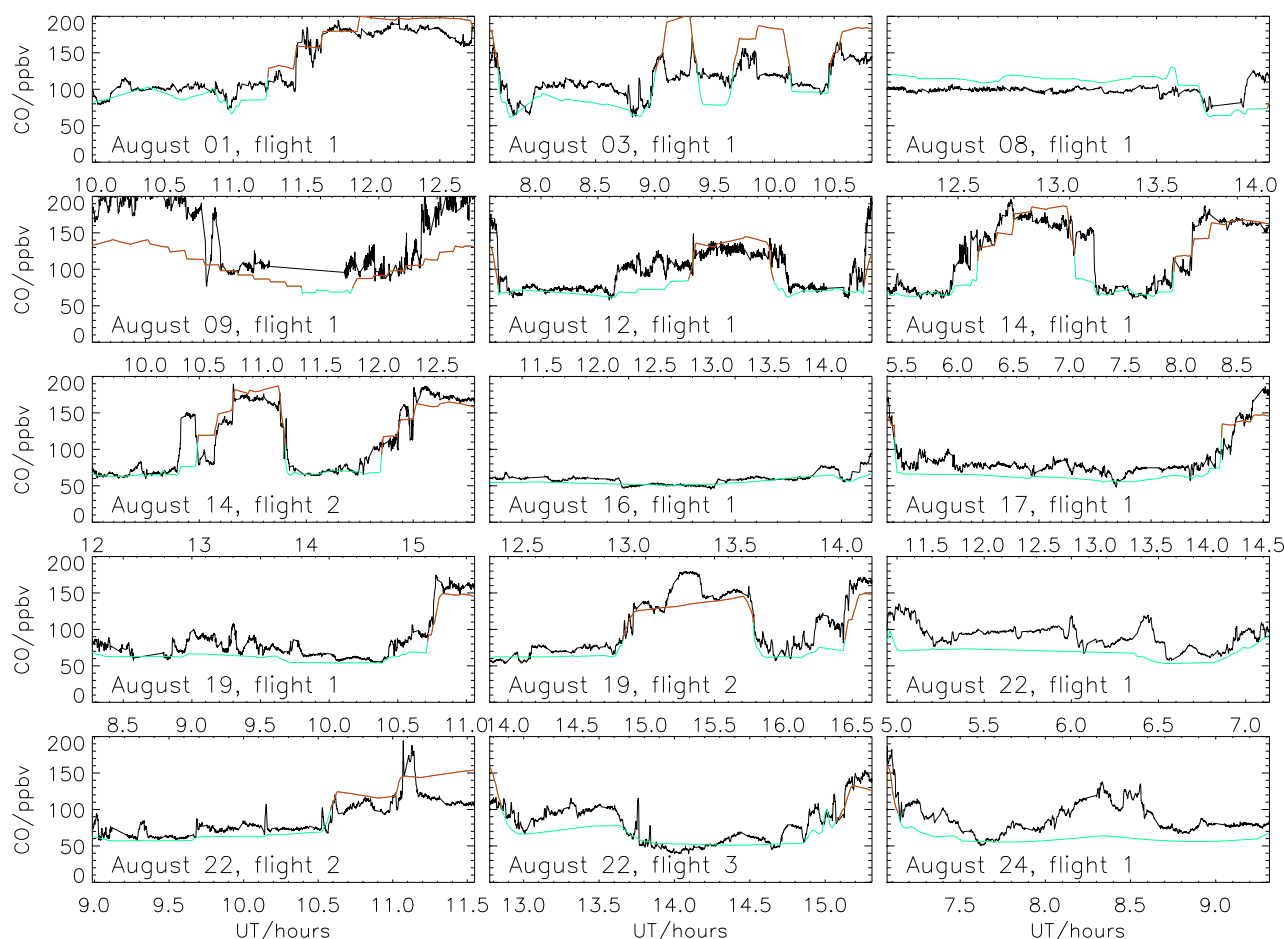
Fig. 1. Observed (black) and TOMCAT model (green and red) CO for each MINOS flight-track. TOMCAT results are coloured red for pressures greater than 700 hPa – in or near the PBL, and green otherwise (see text for explanation).

with coarse scale tracers have been used with success in reproducing observed small scale structure.

Carbon monoxide is used as the test tracer, because it has a relatively simple vertical profile, a long lifetime away from the continental boundary layer and is a common subject for model-measurement comparison. Ozone also has a relatively long lifetime in the upper troposphere, but the O_3 mixing ratio shows extremely large spatial curvature near the tropopause, which is difficult to model.

2 Model and measurements

Carbon monoxide and ozone were measured aboard the German Aerospace Centre (DLR) Falcon aircraft, over the eastern Mediterranean during August 2001, as part of the MINOS campaign. CO was measured by Tunable Diode Laser Spectroscopy, with an accuracy of 2% and precision of 1.5% (Wienhold et al., 1998). O_3 was measured by UV-absorption spectroscopy, to an accuracy of 5% and precision of 2% (Schlager et al., 1997). This study uses measurements averaged over 15 s intervals, which is about 4 km in the horizontal, or equivalent to about 15 m in the vertical according to typical ratios of horizontal and vertical atmospheric scales (Haynes and Anglade, 1997).

Lagrangian back trajectories, arriving at the Falcon flight tracks at one minute intervals, were calculated using the UK Universities Global Atmospheric Modelling program (UGAMP) offline trajectory model (Methven, 1997). The spacing of one minute corresponds to a horizontal resolution about one sixth of that of the meteorological forcing. Methven and Hoskins (1999) showed that high-resolution advection can simulate scales at least six times finer than the forcing resolution, when 6-hourly meteorological analyses are used. Meteorological forcing was provided by T106 analyses from the European Centre for Medium Range Weather Forcasting (ECMWF). These trajectories were used as input to the Cambridge Tropospheric Trajectory model of Chemistry and Transport (CiTTyCAT) (Wild et al., 1996; Evans et al., 2000). CiTTyCAT models photochemical change following trajectories, with a detailed scheme for tropospheric
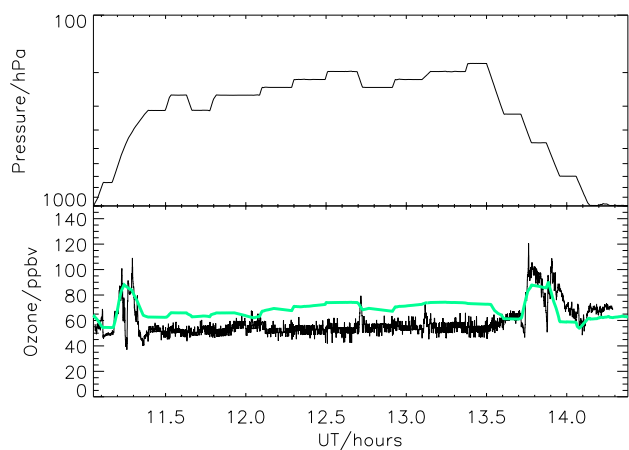
Fig. 2. Flight-track pressure, and ozone from measurements (black) and TOMCAT model (green) for 8 August.

photochemistry, including 90 chemical species and degradation of some hydrocarbons up to C-7, and parameterisations of surface deposition and boundary layer uptake of emissions. Mixing is included only implicitly in the initial tracer fields, and in a simple parameterisation for the vertical spread of surface emissions into the boundary layer. Detail on the use of CiTTyCAT with the UGAMP trajectory model to simulate airborne observations is given by Methven et al. (2001).

Chemical initialization for CiTTyCAT was provided by the TOMCAT 3d CTM, described by Law et al. (1998). The TOMCAT version used had a spatial grid corresponding to the T42 Gaussian grid in the horizontal, and 31 levels in the vertical. This is approximately 2.8° in the horizontal, and vertically 40 hPa in the mid-troposphere and 25 hPa near the tropopause. TOMCAT performs transport using the Prather second-order moments advection scheme (Prather, 1986), and includes a detailed tropospheric photochemistry scheme and parameterisations of boundary layer, convection and lightning processes. Tracer mixing ratios were interpolated to CiTTyCAT trajectory start points by linear spatial interpolation. Forcing is provided by 6-hourly 60-level ECMWF analyses, as for CiTTyCAT, except that for TOMCAT the analyses are truncated spectrally to T42, since there is no benefit in using forcing of resolution higher than that of the CTM. Vertical interpolation of the forcing to the model grid is performed in spectral space.

3 Evaluation of TOMCAT CO fields

Comparisons between TOMCAT and observed CO for each MINOS flight are shown in Fig. 1. TOMCAT CO was interpolated linearly in space, at the model timestep closest to each observation point. TOMCAT results are coloured red for pressures greater than 700 hPa – in or near the PBL, and green otherwise. The relevant feature of the comparison is

that, for pressures less than about 700 hPa, where TOMCAT CO shows a gradient, it will almost always have the correct sign, however, underestimate the magnitude of the observed gradient. The 700 hPa limit is required mostly due to errors in the model's planetary boundary layer (PBL) height and/or due to some overestimation of the PBL CO concentrations. Exceptions are for 1 August, the dip of 20 ppbv at about 10.6 UT (times are given as decimal hours); and for 3 August, the slope from 8.10–8.75 UT. The latter can be associated with numerical mixing of a stratospheric intrusion (the flight of 3 August is discussed further below). Some but not all of the gradient underestimation would be removed if TOMCAT was compared with real atmosphere CO mass averaged over the TOMCAT grid scale, rather than with in-situ flight data. Such a large-scale average is difficult to produce from the available data. The method described above estimates mix-down lifetimes using the structure generated when a trajectory model advects TOMCAT tracer fields. If the TOMCAT tracer gradients are too low, then CiTTyCAT will require longer trajectories, to generate structure of magnitude comparable to that observed, than if TOMCAT gradients were accurate. This leads to an over-estimation of mix-down lifetime. The conclusion is that for the purposes of this method, TOMCAT initialization is useful, above the model PBL, for obtaining upper bound estimates of mix-down lifetimes.

Note that when TOMCAT CO gradients are referred to here, no mention is made of the spatial scale relevant to these gradients. This is because chaotic advection maintains a characteristic relationship between the energy in features of different scales of long lived tracers, above the dissipation scale (see e.g. Nakamura, 2001, and references therein). That is, for long-lived tracers, the relative magnitude of features of different spatial scales is largely controlled by advection. Therefore, the ratio between the magnitudes of features of different spatial scales is expected to be more reliably modelled than the absolute magnitude of a given feature. Also, a characteristic ratio is maintained between vertical and horizontal gradients (Haynes and Anglade, 1997). However, the smallest spatial scales generated by CiTTyCAT will result from stirring of features of the scale of a TOMCAT grid box, so when convection is not important, we are interested in the mix-down from the scale of the TOMCAT grid to the real atmosphere dissipation scale(s).

The approach below only tests the amount of structure in CiTTyCAT results, making no attempt to match specific features in model and data. This means that the assumptions about the CO initialization (from TOMCAT) only concern the statistical distribution of gradient magnitudes. That is, neither the precise positioning of features nor the sign of gradients are important.
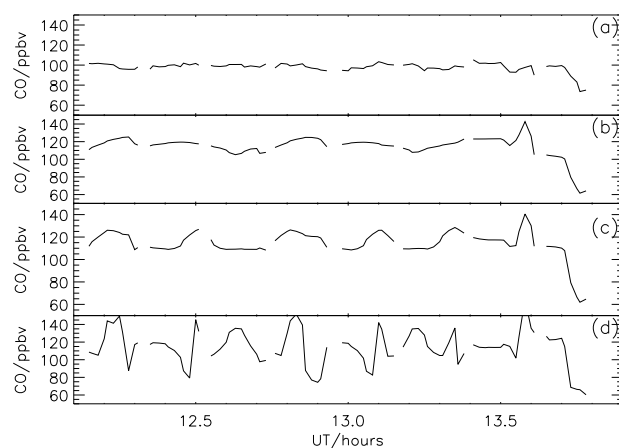
4 Results

4.1 Flight of 8 August 2001

Flight pressure, and ozone from measurements and TOMCAT model for 8 August are plotted in Fig. 2; similar plots for CO are earlier in Fig. 1. The ozone data in particular is quite homogeneous for two hours of the flight, from 11.5–13.5 UT. It is unusual for observed ozone to be so homogeneous over such a large region, so this suggests the possibility of relatively recent mixing. TOMCAT CO (Fig. 1) shows some structure in this region of a similar magnitude to the observations. In the data, relatively low values of O_3 (45–60 ppbv) and NO_y (0.5 ppbv, not shown) may be signatures of clean air mixed up from below. The CO is not low (100 ppbv), but the flight was planned to intercept air rich in biomass-sourced CO from monsoon regions; also, this is the only flight where observed CO is lower than in TOMCAT at these altitudes (Fig. 1). Either side, at lower altitudes (400-600 hPa), peaks in O_3 (Fig. 2) and NO_y (not shown) and a dip in CO (Fig. 1) show good evidence of a stratospheric intrusion, captured and positioned very well by the TOMCAT model.

Observed and CiTTyCAT model CO for 8 August are shown in Fig. 3. Initially, the measurements were available at 15 s intervals and CiTTyCAT results at one minute intervals. In order to intercompare structure fairly, the measurements and CiTTyCAT model results were sampled in two steps. First, the measurement frequency was reduced to that of the model, by selecting only those measurements nearest on the flight track to each model result. Second, in regions where measurements are missing, the coinciding model results were discarded. Note that these plots also focus on only part of the flight – the high altitude central region, which is relatively homogeneous and so a good region for estimating a single mixing time-scale. The same procedure was applied for the other flights investigated below. Model calculations are shown for trajectory calculations initialised from TOMCAT fields at 18 UT on 7 August, 6 August and 4 August, trajectory lengths of less than one, two and four days. Each curve is plotted on a separate axis so that structure is clear.

The CiTTyCAT results show that even back trajectories of less than one day result in over-estimation of the structure in the data. Two- and four-day back trajectory results emphasise this. This suggests a mixdown lifetime, relative to the TOMCAT grid spatial scale, of less than one day. Over this timescale the back trajectories originate from central north Africa; earlier, the air was brought rapidly from the east.

The short mixing timescale and observed tracer concentrations may be indicative of recent convection over north Africa, mixing relatively clean air up from below, and homogenising the tracer distribution through turbulent mixing. However, there is no available independent supporting evidence, so it possible that this result is affected by errors in the trajectory model and/or the initial tracer fields from the


Fig. 3. CO from measurements **(a)** and CiTTyCAT model **(b–d)** for 8 August. Model and measurements are sampled at the same temporal frequency, for fair inter-comparison of structure (see text for details). Model results are shown for trajectory lengths of about 1 (b), 2 (c) and 4 (d) days.

TOMCAT Eulerian model. That is, the structure in the modelled CO time series may be incorrect if the trajectory dispersion is to large, or if initial fields taken from the TOMCAT model show excessively strong spatial gradients.

Scheeren et al. (2003) and Roelofs et al. (2003) use numerical models to infer a Southeast Asian origin for the air observed in this flight. The above suggestion of relatively recent mixing (homogenisation) does not necessarily conflict with this, since it is unclear to what extent homogenisation would affect the bulk origin of the air. Convection may be viewed as a local column of rising air which entrains and mixes turbulently with the surroundings, being progressively diluted as it ascends. Higher up in the column, the proportion of air originating from low level is smaller than lower down in the column. Hence, it is entirely possible for an air 'parcel' to enter a convective region, be mixed – homogenised – locally with air of not dissimilar origin, then exit to undisturbed air. That is, for air exiting from the top of a convective column, the proportion of this air which has been brought up from the bottom of the column may well be small. Hence, this air may be locally homogenised without a large change in its bulk origin. Scheeren et al. (2003) and Roelofs et al. (2003) deal with the bulk origin of the observed air, which is not automatically drastically changed by local homogenisation in the top of a convective column. The extent of these processes for a possible convective event cannot really be estimated using results from a single flight. This will be highly case dependent and would require much greater understanding of the processes involved. This said, the short mixing timescale derived in this work for 8 August requires independent support, in the absence of which our confidence is low in such a result from a single flight.
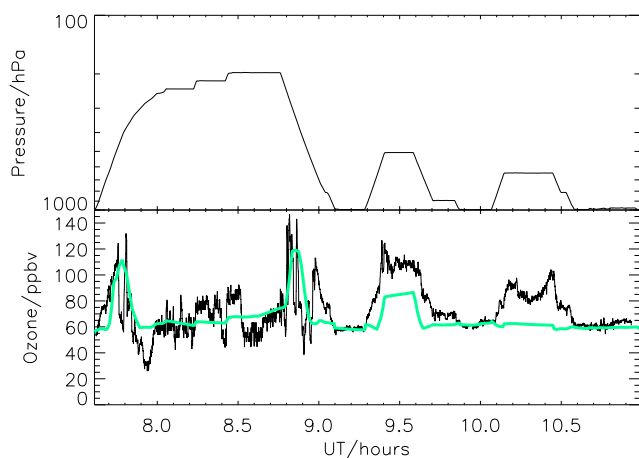
Fig. 4. As Fig. 2, but for 3 August.
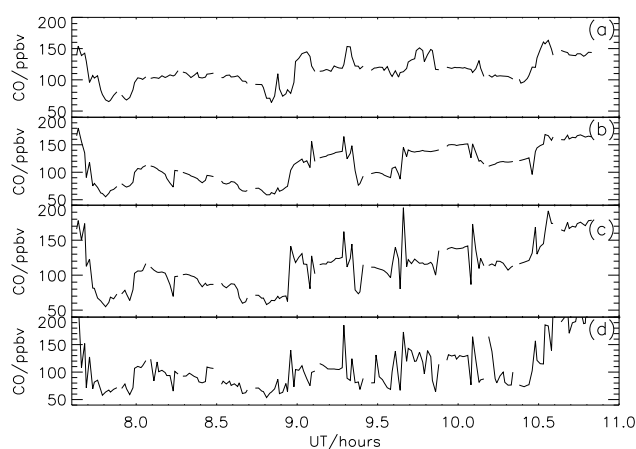
Fig. 5. As Fig. 3, but for 3 August. Model results are shown for trajectory lengths of about 1.5 (**b**), 2.5 (**c**) and 4.5 (**d**) days.

4.2 Flight of 3 August

Data and calculations for 3 August are shown in Figs. 4 and 5. CiTTyCAT model results are shown for trajectory calculations initialised from TOMCAT fields at 18 UT on 1 August, 31 July and 29 July, trajectory lengths of around 1.5, 2.5 and 4.5 days.

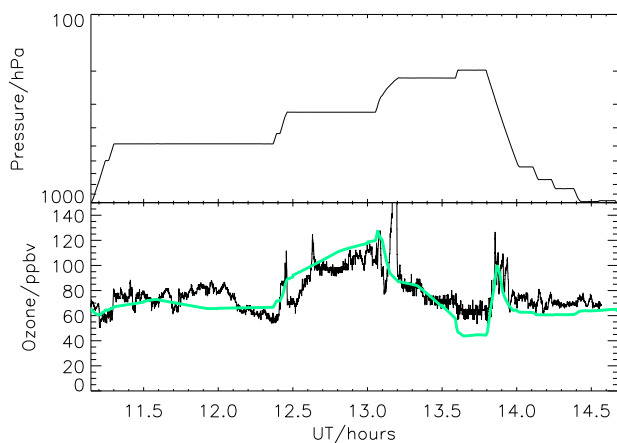### 4.2.1 Interpretation of observed features

This flight is a challenge to model, because it is a multi-level flight which includes a possible influence of asian biomass burning, a stratospheric intrusion, and very distinct but small-scale airmasses at low level. Indeed, this is the flight where TOMCAT has the biggest differences from the data (Fig. 1). The CiTTyCAT trajectory model is able to help in interpretation.

The existence of a stratospheric intrusion seems clear: in the O_3, two main spikes at around 7.75 UT and 8.8 UT appear in both observations and TOMCAT (Fig. 4), co-located with dips in CO (Fig. 1). However, the less prominent structure at high altitude between these features is not reproduced. The 2.5 and 4.5-day CiTTyCAT runs (Fig. 5) reproduce rather detailed structure of the intrusion before 8 UT. The structure after 8.6 UT may be captured, albeit with some misplacement.

At lower altitudes, there are three observed O_3 peaks: at around 9 UT, 9.4–9.6 UT and 10.15–10.45 UT (Fig. 4). The origin of the 9.5 UT peak is discussed in detail. In the TOMCAT 3d CTM such a peak is reproduced with reduced magnitude (Fig. 4). The feature produced by the TOMCAT model is due to the flight track cutting through the very edge of a modelled stratospheric intrusion. Its classification as a stratospheric intrusion is clear from examination of time-series of TOMCAT results. CiTTyCAT Lagrangian model shows a much thinner ozone peak (not shown), due to pollutants uplifted from the top of the PBL. Differences between the models are probably due to mixing in the TOMCAT 3d model broadening the intrusion, and to small differences in PBL height. Back trajectory calculations show the air passing over northern Turkey 1–2 days earlier; less than a day before that they pass in or near the PBL; 10 days before the flight they originate in the UTLS region. Observed CO between 9.4–9.6 UT is too high for a dominant stratospheric signature (Fig. 1), and elevated values of shorter-lived hydrocarbons are also observed, suggesting that air of PBL origin was recently mixed in (Scheeren et al., 2003). On 1 August, around two days before the flight, considerable cloud-to-ground lightning activity over northern and western Turkey was detected by the sferics location system of the United Kingdom Meteorological Office (data is plotted by Wetterzentrale at http://www.wetterzentrale.de), an instrument which detects cloud-to-ground lightning discharges. This observation suggests convective mixing in the real atmosphere, uplifting PBL air. Trajectories arriving at the O_3 peak of 10.15–10.45 UT also pass over northern Turkey and so convective mixing is also implicated for this peak.

The low-altitude CO data also shows complicated structure (Fig. 1). There seem to be two CO populations: one of 110–120 ppbv (at around 09:10 and 10:00) and 140–160 ppbv (around 9.1 UT, 9.3 UT, 9.8 UT and after 10.5 UT). Back trajectories show the low-altitude air coming from the north, and earlier from northern Europe, remaining in the boundary layer. Very short CiTTyCAT integrations, initialised from the TOMCAT 3d CTM only 1.5 days earlier, improve the comparison, on average, with data (Fig. 5), suggesting that TOMCAT was better away from the measurement site. For boundary layer air, the best comparison is obtained when CiTTyCAT is initialised with relatively "clean" air just north west of the European continent, suggesting that in this case CiTTyCAT does a better job of simulating the pick-up of pollution over Europe. For the data taken after 10.5 UT, the trajectories reside rather longer over northern
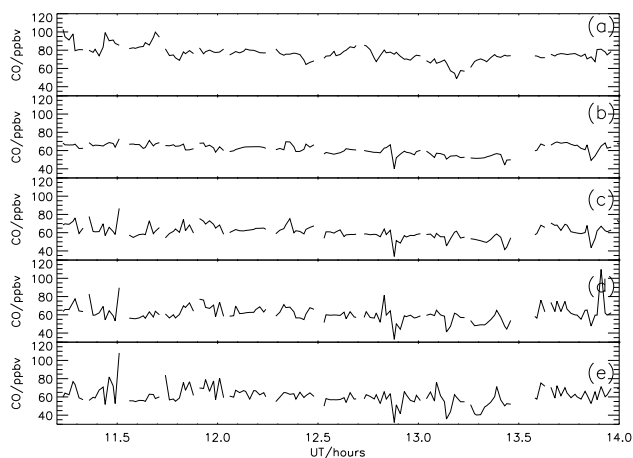
Fig. 6. As Fig. 2, but for 17 August.

Fig. 7. As Fig. 3, but for 17 August. Model results are shown for trajectory lengths of about 5 **(b)**, 7 **(c)**, 9 **(d)** and 11 **(e)** days.

Europe than those for most of the other boundary layer observations, so the former show rather higher CO. This explanation may also apply to the other observed CO peaks over 140 ppbv, but the flight intercepts them too briefly for certainty. However, there is some hint that these peaks are reproduced, if slightly misplaced, at least in the 2.5-day integration.

4.2.2 Mixing timescales

Estimation of mix-down lifetime is done with caution here. The high altitude part of the flight before about 8.9 UT is not considered, because small misplacements of the stratospheric intrusion could cause problems. For the rest, some confidence is given by the fact that CiTTyCAT captures the main properties and even some fine structure of the data for runs of 2.5 and 4.5 days (Fig. 5). This suggests that the TOMCAT fields used to initialise these trajectories were reasonable. That is, although a direct comparison between TOMCAT and observations at the actual measurement points shows TOMCAT performing less well than usual, when TOMCAT was used to initialise the above short trajectories, the results were much more satisfactory. For the 2.5-day run, structure is seen that is not just large in amplitude, but also small in spatial scale compared to that in the data. An upper bound mixing lifetime of 2.5 days is chosen. This short time-scale is consistent with the evidence for recent mixing, either in the boundary layer or convection above. Note that this result is insensitive to photochemical evolution and surface exchange calculated along the trajectories. That is, it was found that if CO was treated as a passive tracer, this did not affect the mix-down timescales derived, since the slow CO photochemistry does not have much influence at small spatial scales. The results presented correspond to full photochemical calculations.

4.3 Flights of 16, 17, 22a, 22c and 24 August

Data and calculations for 17 August are shown in Figs. 6 and 7. Model results are shown for trajectory calculations initialised from TOMCAT fields at 18 UT on 12, 10, 9 and 7 August, trajectory lengths of around 5, 7, 9 and 11 days respectively. The 11-day trajectories originate from a broad region over the North Atlantic and North America, mostly between 100–600 hPa.

For this flight, we examine only the part of the flight for pressures lower than 700 hPa, between about 11.25 UT and 14 UT (Sect. 3). The situation is much simpler than for 3 August, and TOMCAT is able to capture the basic features of O_3 (Fig. 6) and the large scale gradient of CO (Fig. 1) quite well, albeit with an offset.

The back trajectory runs (Fig. 7) show very similar mean values to TOMCAT, with the same large-scale gradient – a consistency that gives some confidence. The relatively simple flight plan and observed air masses give a long time-series with plenty of small-scale structure to allow a reasonable mix-down lifetime estimate. Here, 5-day back trajectories are required to get even close to the amount of structure observed. The 7-day run has possibly a small overestimate, while the 11-day run clearly has too much fine-scale structure.

The comparison was quantified using the Kolmogorov-Smirnov (KS) numerical test (see applications by Fairlie et al., 1997; Dragani et al., 2002). Briefly, the KS test indicates whether two datasets have the same statistical distribution. For the current application, this means that only the amount of structure is compared, so the timing of features along the flight-track has no effect on the result. Also, this test makes no assumption about the form of the statistical distribution. The KS test produces a P-value between 0 and 1, with higher numbers indicating a larger likelihood of a match
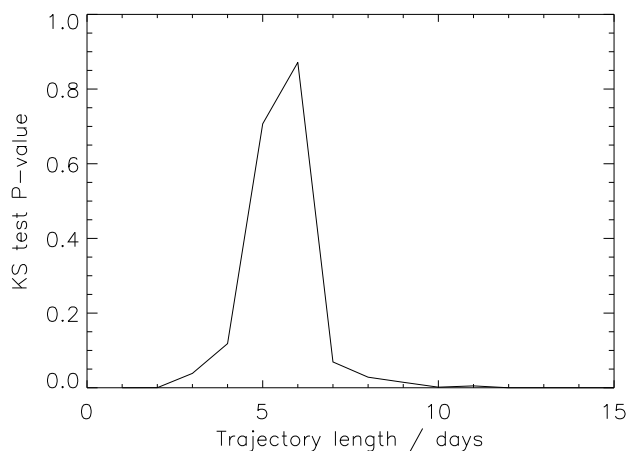
Fig. 8. KS test P-values comparing residual distributions of model results and measurements, for 17 August, as a function of model trajectory length (see text for details).
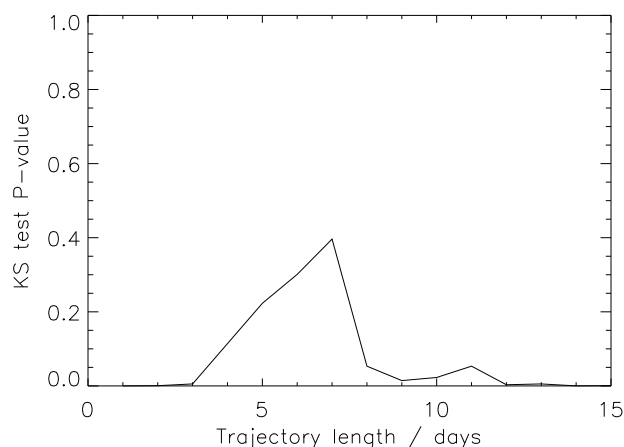

Fig. 9. As Fig. 7, but for 16 August.

between the distributions. The KS test was applied to residual distributions prepared as follows. Each time-series of observations or model results was de-trended, by applying a five minute boxcar average, and then subtracting the smoothed dataset from the original. The resulting residual distributions of data and model results describe the small-scale structure – those features which grow strongly for longer model trajectories. Figure 8 plots KS test P-values for comparisons between model and measurement time-series', as a function of model trajectory length. The best match of residual distributions is indicated for trajectories of 5–6 days, while for 7 days the match is much worse, due to an excess of small-scale structure in the model. Hence, 7 days is taken as an upper bound estimate of the mix-down lifetime for the flight of 17 August.

This longer lifetime is consistent with the trajectories remaining above the PBL, and there is no evidence of recent convection. The same time-scale results are obtained if CO is treated as a passive tracer, as is the case for all the flights studied in this work.

Observations and CiTTyCAT model results for 16 August, the first and third flights of 22 August, and the flight of 24 August, are shown in Figs. 9, 11, 13 and 15. Corresponding plots of KS test P-values are given in Figs. 10, 12, 14 and 16. These are the remaining MINOS flights which featured measurements almost exclusively well above the PBL, and so are appropriate subjects for the above method. They all measured mid-upper tropospheric and some lower stratospheric air transported from the north Atlantic and northern America, in common with the flight of 17 August. For flight c of 22 August, CiTTyCAT shows a large peak at 13.6hr; this is due to trajectories originating from the PBL, and is not apparent in the TOMCAT Eulerian model because this feature is too small to be maintained on the model grid. Fol-
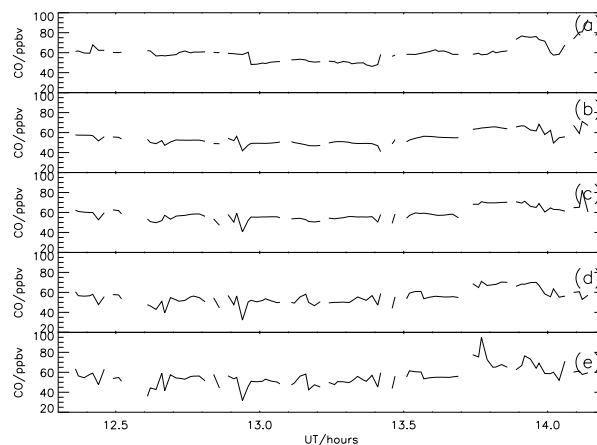

Fig. 10. As Fig. 8, but for 16 August.

lowing the approach described above, mix-down lifetime upperbounds were chosen as follows: 8 days, 7 days, 9 days and 6 days for the flights of 16, 22a, 22c and 24 August, respectively. Note that Fischer et al. (2002) found signatures of recent deep convection for short segments of flight c of 22 August, by looking at observed concentrations of multiple trace species. However, the flight segments for which they identify convective influence are of about 8, 3 and 2 min duration, which is much too short to be detected by the above method of estimating mixing timescales.
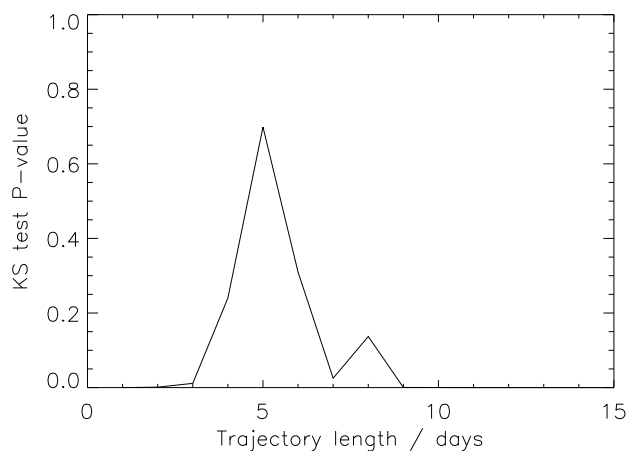
4.3.1 Tolerence with respect to initialization errors

The above results are reliant on the CO initialization, provided by the TOMCAT 3d CTM. The assumption is that TOMCAT CO spatial gradients underestimated the real atmosphere (see Sect. 3). Here, we test how much this assumption can be relaxed for the five similar flights (16, 17, 22a, 22c and 24 August) if a slightly larger upper bound of 11
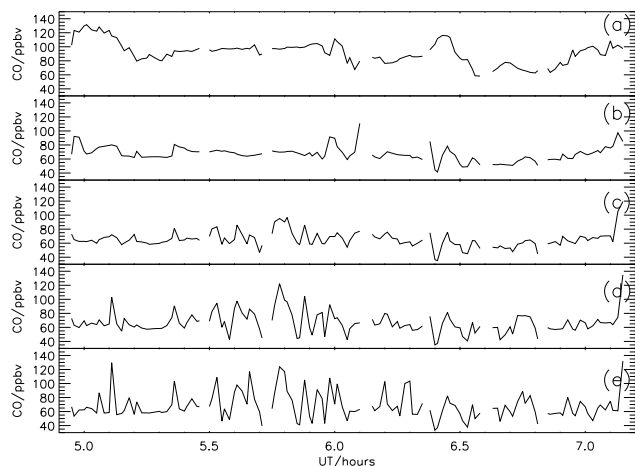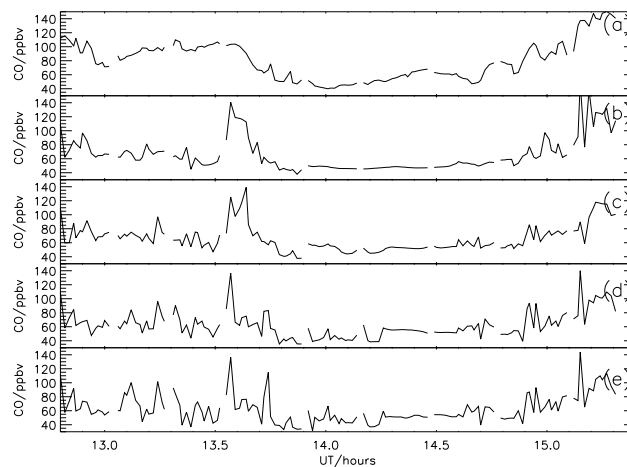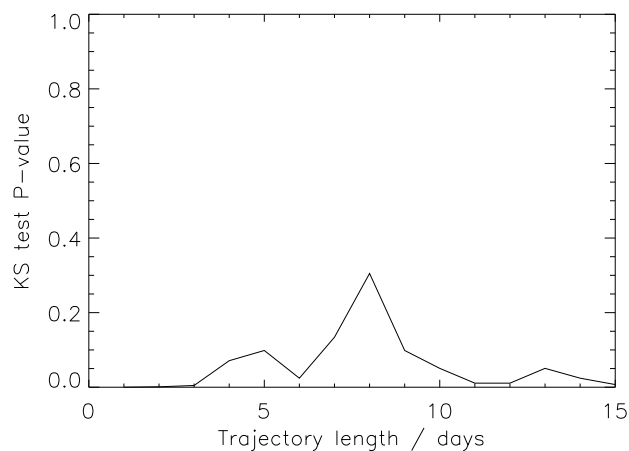
Fig. 11. As Fig. 7, but for 22a August.

Fig. 13. As Fig. 7, but for 22c August.

Fig. 12. As Fig. 8, but for 22 August, flight a.

Fig. 14. As Fig. 8, but for 22 August, flight c.

days is chosen for the mix-down timescale. The question addressed is, if an upper bound of 11 days is accepted as valid for these flights, how large could the errors in TOMCAT CO be? This was quantified using the data and 11-day model results as plotted in Figs. 7–15, i.e. after the datasets had been sub-sampled as described above (Sect. 4.1). Each time-series was de-trended, by applying a five minute boxcar average, and then subtracting the smoothed dataset from the original. The resulting residual distributions of data and 11-day model describe the small-scale structure – those features which grow strongly for longer model trajectories. For CiT-TyCAT, the amplitude of this small-scale structure depends on the spatial gradients in the initialization, since small-scale features are produced by stirring large-scale gradients.

The residual distributions for the measurements were then scaled by factors between one and six. The scale factor α which produced the best match between modelled and (scaled) measured residuals was found for each flight. If

we propose that 11 days is the correct mix-down lifetime, and that the initialization (taken from TOMCAT) is the only source of error, then α is the factor by which TOMCAT CO gradients would have to over-estimate those in the real atmosphere.

Figure 17 plots KS test P-values for each flight as a function of the factor by which the measured residuals were scaled. This shows that scale factors of at least two are required for the best match between modelled and scaled measured residuals. Hence, 11 days overestimates mix-down lifetime for these five flights, unless the spatial gradients in TOMCAT CO overestimate the real atmosphere by factors of at least two.

4.3.2 Sensitivity to the mixing spatial scale

The timescales in this work are appropriate for a specific mixing spatial scale – the grid resolution of the Eulerian

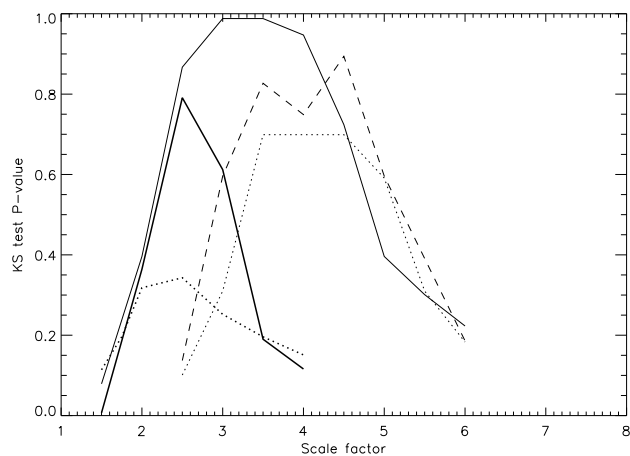**Fig. 15.** As Fig. 7, but for 24 August.

Fig. 16. As Fig. 8, but for 24 August.

Fig. 17. KS test results comparing residual distributions for 11-day model results and scaled observations. The abscissa is the scaling factor applied to the observed residual distribution (see text for details). Thin solid line, August 16; thin dotted line, 17 August; thin dashed line, 22 August flight a; thick solid line, 22 August flight c; thick dotted line, 24 August.

smaller effect than estimated above using advective stretching timescales. This can be explained in part by the recognition that for Eulerian CTMs such as TOMCAT, the grid resolution is the minimum possible resolution for the calculated tracer fields, while the effective resolution will be larger. Effective resolution in this case means the smallest spatial scale that the model is actually able to resolve. If the effective resolution is larger than 2.8°, then smoothing will have a smaller effect than anticipated.

4.3.3 Applicability to mixed Eulerian-Lagrangian models

An indication was sought of how applicable the above results are to the mixed Eulerian-Lagrangian models. The mixed Eulerian-Lagrangian models of interest here perform Lagrangian advection, then apply mixing at the Eulerian grid scale, with a set relaxation timescale. That is, each trajectory mixing ratio is relaxed back to the Eulerian grid mean with the chosen timescale. An approximation to this type of model may be obtained by an appropriate linear combination of CiTTyCAT calculations of different trajectory lengths. This was done for passive - non-chemical integrations, since it was found earlier that the slow CO chemistry has little effect on the small-scale structure. A passive CiTTyCAT integration of length t days advects the low-resolution TOMCAT CO for t days. Thus, a linear combination of passive CiTTy-CAT results of different trajectory lengths t_i, with weighting factors which decay exponentially with t_i, is equivalent to a model which performs Lagrangian advection with a relaxation back to the large-scale mean. The timescale of this relaxation is determined by the exponential decay timescale of the weighting factor. Such summations were performed

tracer fields used to initialise the CiTTyCAT trajectory model. However, the mixing timescale will increase with increasing mixing spatial scale. To obtain timescales appropriate for different mixing spatial scales, then numbers reported above could be scaled roughly according to the stretching timescale of 3.3 days reported by Methven et al. (1999) for trajectories over northern Europe. That is an e-fold reduction of mixing grid length-scale would be expected to require a reduction of the mix-down lifetime by about 3 days. This estimate was tested, by repeating the above experiments but with initial Eulerian fields of degraded spatial resolution. This was done for the five similar flights of August 16, 17, 22a, 22c and 24. The TOMCAT fields used above were smoothed by 2D boxcar averages, reducing the original 2.8° resolution by factors of three and nine – leading to resolutions of 8.4° and 25.2° respectively. The effect was to increase the mix-down time estimate by 0–1.5 days for a smoothing factor of three, and 2–3 days for a smoothing factor of 9. This is a

over integrations of trajectory length 0–20 days, for the five flights where recent convection is not implicated. The results were compared to the observations using the KS test as described earlier, for different relaxation timescales. The optimum relaxation timescale T_r was defined as that with the peak KS P-value. This may be compared with T_s, defined as the equivalent timescale – that with the peak KS P-value – derived using single trajectories, as in the main part of this paper (Sect. 4.3). For three of the flights, T_r was well defined and within one day of T_s. For the other two flights, T_r was not well defined, because convective mixing within TOMCAT affected the CO concentrations of trajectories more than about 14 days long. Thus, where this method is applicable, it is consistent with the results of Sect. 4.3. This indicates that the main results of this paper are approximate estimates of e-folding mixing lifetime upper bounds for the hybrid Eulerian-Lagrangian models.

4.3.4 Discussion

Timescales of the order of a week are comparable to that of the observed cross-Atlantic transport of Northern American boundary layer air reported by Stohl and Trickl (1999). They are also consistent with evidence of ozone peaks, linked to stratospheric intrusions, surviving for more than 10 days (Bithell et al., 2000) in the troposphere. The tropopause ozone gradient is very large, and it is not clear how many e-folding lifetimes would be required for a particular stratospheric intrusion to lose its ozone signature. The timescales derived above are of course specific to a specific region and time of year, which is a problem in applying them to global models, although this is always the case when comparing global models with the results of such measurement campaigns. The method gives an idea of mixing timescales for a particular region; it is a method which may be applied to other campaigns to get wider coverage.

The mixed Eulerian-Lagrangian models STOCHEM (Stevenson et al., 1998) and ATTILA (Reithmeier and Sausen, 2002) are global 3d models. Their mixing timescales are chosen to achieve low numerical diffusivity rather than to accurately simulate small-scale structure. Numerical diffusivity is expected to vary as L^2/T, where L is the length scale of the mixing box, and T is the mixing lifetime. STOCHEM, has large mixing boxes to enable extremely long integrations and therefore needs a long mixing timescale – around 400 days. Note also that STOCHEM includes a convection scheme, which will introduce further tropospheric mixing. ATTILA, however, has mixing boxes comparable in size to those of this study, and uses a lifetime of 20 days in the troposphere.

5 Conclusions

A technique has been demonstrated for estimating mixing time-scales from in-situ data, using a Lagrangian model initialised from an Eulerian CTM. This method was applied to airborne CO observations taken during the MINOS campaign. The time-scales derived are applicable to the family of hybrid Lagrangian-Eulerian models, which perform Lagrangian advection and impose Eulerian mixing between trajectories. Such models have a mix-down lifetime as a free parameter, so it is important to find ways of estimating this parameter independently.

Lagrangian tracer-advection models are generally described as including no mixing processes, however in most applications tracer mixing is implicitly included through their initialization from low resolution gridpoint fields. The mixing spatial scale is determined by the initialization, in particular by the resolution of the gridpoint fields. The mixing time-scale corresponds to the trajectory length. That is, trajectory models initialised from Eulerian tracer fields implicitly have mixing at the spatial scale of the Eulerian initialisation, imposed over the timescale of the trajectory length. Thus choosing a trajectory length is equivalent to selecting a mix-down lifetime. This choice can be made by comparing Lagrangian model results with in-situ observations, for a long lived tracer. If the tracer initialization is a reasonable low-resolution approximation to the real-atmosphere equivalent, then the result estimates the mix-down lifetime required for a hybrid Lagrangian-Eulerian model to reproduce the amount of small-scale structure observed in the real atmosphere. Further, if the advective dispersion of the trajectories is realistic, then the result is an estimate of mix-down lifetime in the real atmosphere.

The method is most appropriate for relatively homogeneous regions, so that small-scale structure is easily distinguished. More confidence is given in the result when reasonably broad regions are examined, so that plenty of small-scale structure is generated in the model.

Physical interpretation of the mix-down lifetime is restricted since the mechanism for mixing in the real atmosphere differs from that in the models described here. In the models, mixing is applied at the large Eulerian grid scale and is then stretched to small scale by Lagrangian advection. In the real atmosphere advection stretches large features, then mixing occurs at small scales. The numerical model approach of large scale mixing is dictated by computational limitations. However, it appears that this approach can be reasonable in some situations, since Lagrangian models initialised with coarse scale tracers have been used with success in reproducing observed small scale structure.

Carbon monoxide was chosen as the test tracer, because it has a long photochemical lifetime and is a common subject for model-measurement comparison. Ozone also has a relatively long lifetime in the upper troposphere, but is unsuitable for the above estimates because the O_3 mixing ratio shows

extremely large spatial curvature near the tropopause, which is difficult to model. An advantage of the method is that for the flights studied above, with CO as the test tracer the results are very insensitive to photochemical change calculated along the trajectories. Thus, errors in model photochemistry are unlikely to affect the conclusions.

In the experiments described above, the TOMCAT 3-d CTM provided CO initialization. The MINOS campaign featured flights of the DLR falcon aircraft. The variety of flight configurations allowed tests of the TOMCAT CO tracer gradients, which underestimate those in the real atmosphere, above the model planetary boundary layer. For this reason, the mix-down lifetimes derived above are treated as upper bound estimates only.

Seven flights were examined, with mix-down lifetime upper bounds of 1 day for 8 August, 2.5 days for 3 August and 6–9 days for the five flights of 16, 17, 22a, 22c and 24 August. Thus, five of the flights have rather similar mix-down lifetime estimates. Recent convective and boundary layer mixing are likely explanations of the short time-scale for 3 August. Recent convective mixing is possible for 8 August, although independent supporting evidence was not available, so model error cannot be ruled out. Indeed, this method is more appropriate for getting an idea of typical mixing timescales corresponding to a particular region and time of year, using multiple flights, rather for strong statements about individual flights.

For the flight of 3 August, the observed air shows much complexity. It shows considerable structure due to a stratospheric intrusion, PBL air uplifted by convection and/or advection, and different PBL air histories. Here, the models are used more generally to interpret the data in support of MINOS, and illustrate where more caution is required with the above method of estimating mix-down lifetimes.

For the five flights with similar mix-down lifetimes, of 6–9 days, the sensitivity to errors in the CO initialization was tested. Numerical comparisons were made of the small-scale structure in the observations and in model results for 11 day trajectories. It was shown that the slightly weaker upper bound of 11 days overestimates mix-down lifetimes for these five flights unless the spatial gradients in TOMCAT CO are too large by factors of at least two. These lifetimes are consistent with observed long-range transport across the Atlantic. Existing mixed Lagrangian-Eulerian models use longer lifetimes in order to limit numerical diffusivity.

Realistic and representative mixing time-scales are difficult to estimate. The approach presented above offers some possibility to assist characterizing atmospheric mixing times. Further development work will aim to further constrain the errors in initilisation, and to test the applicability of simple mixing with these timescales for the CiTTyCAT photochemical transport model. It may be necessary to use smaller mixing grid boxes, to limit numerical diffusivity. The timescales in this work can be scaled roughly according to the stretching timescale of 3.3 days reported by Methven et al. (1999) for

trajectories over northern Europe. That is, an e-fold reduction of mixing grid length-scale would be expected to require a reduction of the mix-down lifetime by about 3 days. Tests using initial Eulerian fields of degraded resolution showed a smaller dependence on spatial resolution, although this may be due to the fact that the effective, as opposed to grid resolution of the TOMCAT fields is uncertain.

References

Bithell, M., Vaughan, G., and Gray, L. J.: Persistence of stratospheric ozone layers in the troposphere, Atmos. Environ., 34, 2563–2570, 2000.

Dragani, R., Redaelli, G., Visconti, G., Mariotti, A., Rudakov, V., MacKenzie, A. R., and Stefanutti, L.: High-resolution stratospheric tracer fields reconstructed with Lagrangian techniques: A comparative analysis of predictive skill, J. Atmos. Sci., 59, 1943–1958, 2002.

Evans, M. J., Shallcross, D. E., Law, K. S., Wild, J. O. F., Simmonds, P. G., Spain, T. G., Berrisford, P., Methven, J., Lewis, A. C., McQuaid, J. B., Pilling, M. J., Bandy, B. J., Penkett, S. A., and Pyle, J. A.: Evaluation of a Lagrangian box model using field measurements from EASE (Eastern Atlantic Summer Experiment) 1996, Atmos. Environ., 34, 3843–3863, 2000.

Fairlie, T. D., Pierce, R. B., Grose, W. L., Lingenfelser, G., Loewenstein, M., and Podolske, J. R.: Lagrangian forecasting during ASHOE/MAESA: Analysis of predictive skill for analyzed and reverse-domain-filled potential vorticity, J. Geophys. Res.-Atmos., 102, 13 169–13 182, 1997.

Fairlie, T. D., Pierce, R. B., Al-Saadi, J. A., Grose, W. L., Russell, J. M., Proffitt, M. H., and Webster, C. R.: The contribution of mixing in Lagrangian photochemical predictions of polar ozone loss over the Arctic in summer 1997, J. Geophys. Res.-Atmos., 104, 26 597–26 609, 1999.

Fischer, H., de Reus, M., Traub, M., Williams, J., Lelieveld, J., de Gouw, J., Warneke, C., Schlager, H., Minikin, A., Scheele, R., and Siegmund, P.: Deep convective injection of boundary layer air into the lowermost stratosphere at midlatitudes, Atmos. Chem. Phys. Discuss., 2, 2003–2019, 2002.

Haynes, P. and Anglade, J.: The vertical-scale cascade in atmospheric tracers due to largescale differential advection, J. Atmos. Sci., 54, 1121–1136, 1997.

Haynes, P. and Shuckburgh, E.: Effective diffusivity as a diagnostic of atmospheric transport 1. Stratosphere, J. Geophys. Res.-Atmos., 105, 22 777–22 794, 2000a.

Haynes, P. and Shuckburgh, E.: Effective diffusivity as a diagnostic of atmospheric transport 2. Troposphere and lower stratosphere, J. Geophys. Res.-Atmos., 105, 22 795–22 810, 2000b.

Law, K. S., Plantevin, P. H., Shallcross, D. E., Rogers, H. L., Pyle, J. A., Grouhel, C., Thouret, V., and Marenco, A.: Evaluation of modeled O_3 using Measurement of OZone by AIrbus in-service airCraft (MOZAIC) data, J. Geophys. Res.-Atmos., 103, 25 721–25 872, 1998.

Lee, A. M., Roscoe, H. K., Jones, A. E., Haynes, P. H., Shuckburgh, E. F., Morrey, M. W., and Pumphrey, H. C.: The impact of the mixing properties within the Antarctic stratospheric vortex on ozone loss in spring, J. Geophys. Res.-Atmos., 106, 3203–3211, 2001.

Manney, G. L., Zurek, R. W., Lahoz, W. A., Harwood, R. S., Gille, J. C., Kumer, J. B., Mergenthaler, J. L., Roche, A. E., O'Neill, A., Swinbank, R., and Waters, J. W.: Lagrangian transport calculations using UARS data .1. Passive tracers, J. Atmos. Sci., 52, 3049–3068, 1995.

McKenna, D. S., Konopka, P., Grooss, J. U., Gunther, G., Muller, R., Spang, R., Offermann, D., and Orsolini, Y.: A new chemical Lagrangian model of the stratosphere (clams) – 1. Formulation of advection and mixing, J. Geophys. Res.-Atmos., 107, art. no.– 4309, 2002.

Methven, J.: Offline trajectories: Calculation and accuracy, Tech. Rep. 44, UK Univ. Global Atmos. Modelling Programme, Dept. of Meteorol., Univ. of Reading, Reading, UK, 1997.

Methven, J. and Hoskins, B.: The advection of high-resolution tracers by low-resolution winds, J. Atmos. Sci., 56, 3262–3285, 1999.

Methven, J., Berrisford, P., and Hoskins, B.: A Lagrangian climatology for the North Atlantic, Tech. Rep. 9, Hadley Centre, Meteorol. Off., Bracknell, UK, 1999.

Methven, J., Evans, M., Simmonds, P., and Spain, G.: Estimating relationships between air mass origin and chemical composition, J. Geophys. Res.-Atmos., 106, 5005–5019, 2001.

Methven, J., Arnold, S., O'Connor, F., Barjat, H., Dewey, K., Kent, J., and Brough, N.: Estimating photochemically produced ozone throughout a domain using flight data and a Lagrangian model, J. Geophys. Res., accepted, 2003.

Morgenstern, O. and Carver, G. D.: Quantification of filaments penetrating the subtropical barrier, J. Geophys. Res.-Atmos., 104, 31 275–31 286, 1999.

Nakamura, N.: Two-dimensional mixing, edge formation, and permeability diagnosed in an area coordinate, J. Atmos. Sci., 53, 1524–1537, 1996.

Nakamura, N.: A new look at eddy diffusivity as a mixing diagnostic, J. Atmos. Sci., 58, 3685–3701, 2001.

O'Neill, A., Grose, W. L., Pope, V. D., MacLean, H., and Swinbank, R.: Evolution of the stratosphere during northern winter 1991/92 as diagnosed from UK Meteorological Office analyses, J. Atmos. Sci., 51, 2800–2817, 1994.

Pierce, R. B., Fairlie, T. D., Grose, W. L., Swinbank, R., and O'Neill, A.: Mixing processes within the polar night jet, J. Atmos. Sci., 51, 2957–2972, 1994.

Plumb, R. A. and Ko, M. K. W.: Interrelationships between mixing ratios of long lived stratospheric constituents, J. Geophys. Res.-Atmos., 97, 10 145–10 156, 1992.

Plumb, R. A., Waugh, D. W., Atkinson, R. J., Newman, P. A., Lait, L. R., Schoeberl, M. R., Browell, E. V., Simmons, A. J., and Loewenstein, M.: Intrusions into the lower stratospheric Arctic vortex during the winter of 1991–1992, J. Geophys. Res.-Atmos., 99, 1089–1105, 1994.

Plumb, R. A., Waugh, D. W., and Chipperfield, M. P.: The effects of mixing on traces relationships in the polar vortices, J. Geophys. Res.-Atmos., 105, 10 047–10 062, 2000.

Prather, M. J.: Numerical advection by conservation of 2nd-order moments, J. Geophys. Res., 91, 6671–6681, 1986.

Reithmeier, C. and Sausen, R.: Attila: atmospheric tracer transport in a Lagrangian model, Tellus Ser. B-Chem. Phys. Meteorol., 54, 278–299, 2002.

Roelofs, G. J., Scheeren, B., Heland, J., Ziereis, H., and Lelieveld, J.: Distribution and origin of ozone in the eastern Mediterranean free troposphere during MINOS (August 2001), Atmos. Chem. Phys., this issue, 2003.

Scheeren, H., Lelieveld, J., Roelofs, G., Williams, J., Fischer, H., de Reus, M., de Gouw, J., Warneke, C., Holzinger, R., Schlager, H., Klupfel, T., Bolder, M., van der Veen, C., and Lawrence, M.: The impact of monsoon outflow from India and Southeast Asia in the upper troposphere over the Eastern Mediterranean, Atmos. Chem. Phys., this issue, 2003.

Schlager, H., Konopka, P., Schulte, P., Schumann, U., Ziereis, H., Arnold, F., Klemm, M., Hagen, D. E., Whitefield, P. D., and Ovarlez, J.: In situ observations of air traffic emission signatures in the North Atlantic flight corridor, J. Geophys. Res.-Atmos., 102, 10 739–10 750, 1997.

Stevenson, D. S., Collins, W. J., Johnson, C. E., and Derwent, R. G.: Intercomparison and evaluation of atmospheric transport in a Lagrangian model (STOCHEM), and an Eulerian model (um), using Rn-222 as a short-lived tracer., Q. J. R. Meteorol. Soc., 124, 2477–2491, 1998.

Stohl, A. and Trickl, T.: A textbook example of long-range transport: Simultaneous observation of ozone maxima of stratospheric and North American origin in the free troposphere over Europe, J. Geophys. Res.-Atmos., 104, 30 445–30 462, 1999.

Sutton, R. T., MacLean, H., Swinbank, R., O'Neill, A., and Taylor, F. W.: High-resolution stratospheric tracer fields estimated from satellite-observations using Lagrangian trajectory calculations, J. Atmos. Sci., 51, 2995–3005, 1994.

Tan, D. G. H., Haynes, P. H., MacKenzie, A. R., and Pyle, J. A.: Effects of fluid-dynamical stirring and mixing on the deactivation of stratospheric chlorine, J. Geophys. Res.-Atmos., 103, 1585–1605, 1998.

Thuburn, J. and Tan, D. G. H.: A parameterization of mixdown time for atmospheric chemicals, J. Geophys. Res.-Atmos., 102, 13 037–13 049, 1997.

Walton, J. J., MacCracken, M. C., and Ghan, S. J.: A global-scale Lagrangian trace species model of transport, transformation, and removal processes, J. Geophys. Res.-Atmos., 93, 8339–8354, 1988.

Wienhold, F. G., Fischer, H., Hoor, P., Wagner, V., Konigstedt, R., Harris, G. W., Anders, J., Grisar, R., Knothe, M., Riedel, W. J., Lubken, F. J., and Schilling, T.: Tristar – a tracer in situ TDLAS for atmospheric research, Appl. Phys. B-Lasers Opt., 67, 411–417, 1998.

Wild, O., Law, K. S., McKenna, D. S., Bandy, B. J., Penkett, S. A., and Pyle, J. A.: Photochemical trajectory modeling studies of the North Atlantic region during August 1993, J. Geophys. Res.-Atmos., 101, 29 269–29 288, 1996.